Available online at www.sciencedirect.com
SCIENCE DIRECT®
Journal of Organometallic Chemistry 689 (2004) 4611–4623
Journal of Organometallic Chemistry
www.elsevier.com/locate/jorganchem

The reaction of the group-13 alkyls ER_3 (E = Al, Ga, In; R = CH_2t-Bu, CH_2 $SiMe_3$) with the platinum-complex [(dcpe)Pt(H)(CH_2t-Bu)]

Roland A. Fischer [a,*], Dana Weiß [a], Manuela Winter [a], Iris Müller [a], Herbert D. Kaesz [b], Nikolaus Fröhlich [a,b,c], Gernot Frenking [c]

[a] *Fakultät Chemie, Lehrstuhl f. Anorganische Chemie III, Ruhr-Universität Bochum, Universitätsstraße 150, D-44780 Bochum, Germany*
[b] *Department of Chemistry and Biochemistry, UCLA, 607 Charles E. Young Drive East, Los Angeles, CA 90095-1569, USA*
[c] *Fachbereich Chemie, Philipps-Universität Marburg, Hans-Meerwein-Straße, 35032 Marburg, Germany*

Abstract

The reactions of the sterically demanding group-13 alkyls ER_3 (E = Al, Ga, In; R = CH_2 *t*-Bu, CH_2SiMe_3) with the platinum-complex [(dcpe)Pt(H)(CH_2t-Bu)] were re-investigated. The bimetallic compounds [(dcpe)Pt(ER_2)(R)] (**3**: E = Ga, R = CH_2SiMe_3; **5**: E = In, R = CH_2t-Bu; dcpe = bis(dicyclohexylphosphino)ethane) with direct σ(Pt–E) bonds were obtained by oxidative addition of an E-C bond to the coordinatively unsaturated fragment [(dcpe)Pt] produced *in situ* by thermolysis of the starting complex [(dcpe)Pt(CH_2t-Bu)(H)]. The single crystal structure determination reveals a Pt–Ga bond length of 2.376(2) Å and a Pt–In bond length of 2.608(1) Å. All new compounds were characterised by elemental analysis, ^{31}P and ^{195}Pt NMR spectroscopy. Interestingly, the Pt–Ga compound **3** slowly transforms into the platinum alkyl/hydride isomer {(dcpe)Pt(μ_2-H)[$CH_2Si(CH_3)_2$ $CH_2Ga(CH_2SiMe_3)_2$]} (**4**) during crystallization from solution at room temperature. The X-ray single crystal structure analysis revealed both complexes **3** and **4** coexisting in the unit cell in a 1:1 relation. The inaccessibility of analytically pure samples of the Pt–Al complex {(dcpe)Pt[Al(CH_2t-Bu)$_2$](CH_2t-Bu)} (**6**), postulated as intermediate of the reaction of [(dcpe)Pt(H)(CH_2t-Bu)] with Al(CH_2t-Bu) on the basis of ^{31}P and ^{195}Pt NMR data, is attributed to an enhanced tendency to isomerisation into the alkyl/hydride Pt/Al congener of **4**. A brief DFT analysis of the bonding situation of the model complex [(dhpe)Pt($GaMe_2$)(Me)] (**1M**) revealed, that the contribution of π(Pt–Ga) back-bonding is negligible.

1. Introduction

Structural data of the first bimetallic complexes with direct covalent σ(Pt–Ga) and σ(Pt–In) bonds, [(dcpe)Pt{Ga(CH_2t-Bu)$_2$}(CH_2t-Bu)] (**1**) and [(dcpe)Pt{In(CH_2SiMe_3)$_2$}(CH_2SiMe_3)] (**2**), respectively, have been reported as preliminary short communications by Fischer et al. [1,2] more than a decade ago. The original motivation of these studies arose from the idea to use such mixed metal compounds as "single-source" precursors for intermetallic materials predominantly using Metal Organic Vapor Deposition [3,4]. But, because of the involatility of **1** and **2**, the interest into these type of Pt–E compounds ceased. In parallel however, starting by the mid 1990s, heterometallic compounds exhibiting bonds between transition-metals and group-13-metals aluminium, gallium and indium gained more general attention as objects for theoretical studies on metal-metal donor acceptor bonds M ← E including the discussion of π-type backbonding and multiple bond effects [5–8]. This renewed interest in that chemistry was

* Corresponding author. Tel.: +49 234 700 4174; fax: +49 234 709 4174.
E-mail address: rfischer@aci.aci.ruhr-uni-bochum.de (R.A. Fischer).

0022-328X/$ - see front matter © 2004 Published by Elsevier B.V.
doi:10.1016/j.jorganchem.2004.09.059

initiated by the availability of stable low valent, carbene-like compounds E^IR (E = Al, Ga, In; R = Cp^*, $C(SiMe_3)_3$, etc.), pioneered by H. Schnöckel, W. Uhl and others which opened a new field of group-13 transition metal coordination chemistry [4,9]. The new ''metallic'' ligands E^IR (in metaphoric contrast to typical ''none-metallic'' ligands such as phosphanes) revealed a coordination chemistry similar to CO and phosphanes PR_3. For example, we reported on a series of group-13 metal rich platinum compounds of PtE_2 stoichiometry, namely the tetrahedral Pt^0 complexes $[(dcpe)Pt(ECp^*)_2]$ and $[(dcpe)Pt\{EC(SiMe_3)_3\}_2]$ [10a,b] containing the group-13 metal in the formal low oxidation state E^I rather than E^{III} as in the case of the square planer Pt^{II} complexes **1** and **2**. The platinum group-13 metal chemistry is somewhat unique in the sense, that it allows a quite comprehensive study of the coordination chemistry of both fragments, E^IR and $E^{III}R_2$ at the same transition metal centre. This situation is also nicely illustrated by the existence of the homoleptic complexes $[Pt(ER)_4]$ (E = In[$C(SiMe_3)_3$], $GaCp^*$) [10c,d] and the dinuclear cluster $[Pt_2(GaCp^*)_5]$ [10e]. Most recent results on the related series of clusters $M_a(E^ICp^*)_b$ (M = Pd, Pt; E = Al, Ga, In; a = 2, 3) including a discussion of their fluxional behaviour in solution and ligand exchange reactions have been communicated elsewhere [11]. Interestingly, it was found, that low coordinated congeners $[Ni(AlCp^*)_3]$, which are thought to exist as intermediates in the course of the synthesis of the saturated $[Ni(AlCp^*)_4]$, show interesting reactivity and activate aromatic C–H bonds and Si–H bonds, for example [12]. This kind of transition metal aluminium chemistry holds promise for even more unusual observations, as the structures of $[M(AlCp^*)_5]$ (M = Fe, Ru) [13] again turned out to exhibit more complexity as initially thought: Two C–H bonds of the methyl groups of the Cp^*-ligands are activated and the coordination sphere around the metal centres contain only three unchanged Al^I Cp^* ligands besides two Al^{III} centers being linked to M by hydride M–H–Al bridges in addition to M–Al donor acceptor bonds. This situation appears to be quite similar to the complex $[(Cp^*Al)_3Ni(\mu\text{-}H)Al(\eta^1Cp^*)(Ph)]$ mentioned above [12]. In addition, we recently found a related and intriguing example of C–C bond activation most likely taking place at the low valent main group center E (Al, Ga) rather than involving directly the transition metal center in the case of the rearrangement of $[Cp^*Rh(CH_3)_2(ECp^*)]$ into the zwitterionic rhodenocenium/gallanate complexes $[Cp^*Rh\{\eta^5\text{-}C_5Me_4(GaMe_3)\}]$ [14]. Our attention was thus drawn back to our older work on Pt–ER_2 species (exhibiting E^{III} rather than E^I) mentioned above in order to now study in more detail the reactivity of the group-13 alkyls ER_3 (E = Al, Ga, In; R = CH_2t-Bu, CH_2SiMe_3) with the platinum complex [(dcpe)Pt(H)(CH_2t-Bu)], particularly addressing the synthesis and spectroscopic characterization of the aluminium congener of **1** and **2**, namely [(dcpe)Pt{$Al(CH_2t\text{-}Bu)_2$}(CH_2t-Bu)] (**6**) and aiming at a more general comparison of the Pt^{II}–E^{III} bonded systems with the related Pt^0–E^I examples $[(dcpe)Pt(ER)_2]$ (R = Cp^*, $C(SiMe_3)_3$) [10a,b].

2. Results and discussion

2.1. Synthesis

We reinvestigated the formation of the previously reported compounds **1** and **2** and synthesised the new congeners **3**, **5** and **6** by the reaction outlined in Scheme 1. Thermolysis of the platinum alkyl/hydride complex [(dcpe)Pt(H)(CH_2t-Bu)] in solution at 70–90 °C following a procedure described by Whitesides et al. results in the generation of the intermediate [(dcpe)Pt] via a rate determining, unimolecular neopentane elimination. This highly reactive and electronically unsaturated 14e fragment is well known to undergo various oxidative addition reactions including the activation of sp^3-C–H bonds and the addition of Si–C bonds [15]. According to Scheme 1 a formal oxidative addition of an E–C bond of ER_3 (E = Al, Ga, In; R = CH_2t-Bu; and E = Ga, In, R = CH_2SiMe_3) to [(dcpe)Pt] is possible and the Pt–Ga and Pt–In compounds **1**–**3** and **5** were quantitatively formed (as confirmed by in situ ^{31}P NMR spectroscopy) and isolated as crystalline, analytically pure samples with satisfying yields around 60–80%. It should be noted, that a significant excess of ER_3 (about 2-fold) is necessary for a selective formation of the Pt–E complexes. When the reaction was conducted with a 1:1 stoichiometry of [(dcpe)Pt(H)(CH_2t-Bu)] and ER_3 in a suitable hydrocarbon solvent (such as methylcyclohexane) the undesired CH-activation of the solvent took place to a significant extent (observed by ^{31}P NMR) and the isolation of pure products was impossible. The isolation of a pure sample of the aluminium homologues **6**–**7**, and the growth of single crystals suitable for X-ray diffraction studies, failed to our surprise and disappointment. But the existence of **6** is substantiated by NMR spectroscopy (see the discussion below). In addition, when simple alkyls ER'_3 were employed with the small alkyl groups R′ = Me, Et, *i*-Bu rather than $E(CH_2t\text{-}Bu)_3$ and $E(CH_2SiMe_3)_3$ the exchange of the alkyl and hydrido group at the Pt centre was observed without hints for C–H side products. The quantitative formation of symmetrically substituted $[(dcpe)PtR'_2]$ occurred (^{31}P NMR) and no stable complexes of the type $[(dcpe)Pt(ER'_2)(R')]$ could be isolated or detected. Sterically demanding groups R (without β-H-atoms) seem to be a stringent requirement to obtain the Pt–E bonded complexes using our synthetic strategy of trapping the $[L_2Pt]$ fragment.

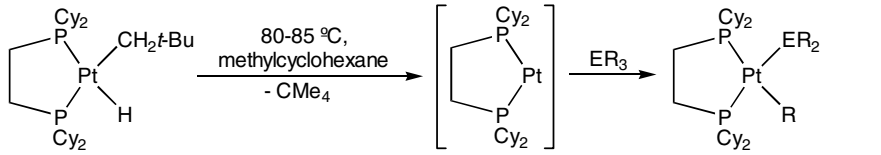

1 (E = Ga, R = CH $_2$*t*-Bu)
2 (E = In, R = CH $_2$SiMe$_3$)
3 (E = Ga, R = CH $_2$SiMe$_3$)
5 (E = In, R = CH $_2$*t*-Bu)
6 (E = Al, R = CH $_2$*t*-Bu)

Scheme 1.

Interestingly, in the case of monosilyl groups (CH_2SiMe_3) at the gallium centre instead of neopentyl (CH_2*t*-Bu) a consecutive reaction gains importance, leading to the formation of a hydride isomer of **3** without a direct Pt–Ga bond as is shown for compound **4**. The monosyl substituted Pt–Ga compound [(dcpe)Pt{$Ga(CH_2SiMe_3)_2$}(CH_2SiMe_3)] (**3**) partly rearranges into a complex of the formula [(dcpe)Pt(μ_2-H){$CH_2Si(CH_3)_2$ $CH_2Ga(CH_2SiMe_3)_2$}] (**4**). We detected this by the very, very slow crystallization of the reaction product within a time span of a number of months (!) at −30 ° C being contained in a tightly sealed vessel. The very same effect can be observed by prolonged heating of the actual reaction mixture after the quantitative formation of **3** (by ^{31}P NMR). However it was not possible to *quantitatively* transform isolated, pure **3** into pure **4** upon heating in methylcyclohexane solution. This indicates, that the isomers **3** and **4** coexist in a temperature dependent equilibrium (But we did not attempt to study this equilibrium quantitatively). Our interest concentrated on the synthesis and structural characterisation of the title compounds and we therefore did not attempt to elucidate the mechanistic details of the reaction of ER_3 and ER'_3 with [(dcpe)Pt(H)(CH_2*t*-Bu)], so far. However, we wish to present a comment on possible mechanistic alternatives. Two reaction pathways are imaginable. One possibility is the *intramolecular* reductive elimination of GaR_3 from complex **3** followed by an *intermolecular* oxidative addition of a γ-C–H bond of the GaR_3 unit to the [(dcpe)Pt] intermediate, which is well known for it's C–H-activating properties. Another pathway includes an *intramolecular* oxidative addition of the γ-C–H bond of the coordinated GaR_2 fragment to the Pt centre, followed by the again *intramolecular* reductive elimination of the $(R)_2Ga[CH_2Si(CH_3)_2CH_2]$ unit under retention of the Pt–C and Pt–H bonds formed in the first step of the rearrangement. If we take into account, that if pure **3** rearranges into **4** and a free intermediate [(dcpe)Pt], this latter species, if formed, would certainly also attack the solvent C–H bonds, as we observed in the case of the 1:1 reaction between GaR_3 and [(dcpe)Pt(H)(CH_2*t*-Bu)], it seems, that a stepwise mechanism involving the reductive elimination of GaR_3, i.e., the reverse of the formation reaction of **3**, is not a very likely explanation of the peculiar rearrangement. We thus favour an intermolecular pathway. It should be noted also, that in case of the compounds E^IR'' (R″ = Cp* and $C(SiMe_3)_3$), which contain a lot of C–H bonds, we did not observe any hints for side products which stem from C–H activation in the periphery of the R″ substituents. The ER″ ligands effectively trap the in situ formed fragment [(dcpe)Pt] to yield the coordinatively saturated 18e tetrahedral complexes [(dcpe)Pt$(ER'')_2$], which proved dissociation stable.

The tendency of the title compounds [(dcpe)Pt(ER_2)(R)] to undergo the described rearrangement rises following the order In < Ga < Al and CH_2-*t*-Bu < CH_2SiMe_3, which was estimated based on in situ ^{31}P and ^{195}Pt NMR studies (see below). So, for both indium compounds **2** and **5** and the neopentyl gallium complex **1** the formation of a hydridic Pt/E complex was not observed. However, this rearrangement is rather important forthe reaction of AlR_3 with [(dcpe)Pt(H)-(CH_2*t*-Bu)] which causes the inaccessibility of pure samples of **6** and **8**. We thus failed to obtain suitable crystals for structure elucidation of the aluminium congeners **6** and **8** of the Ga compounds **1** and **2**. Also, due to the extreme sensitivity to moist air, we failed to obtain satisfactory elemental analysis of **6** and **8**. However, the existence of the aluminium complex [(dcpe)Pt{$Al(CH_2$*t*-Bu$)_2$}(CH_2*t*-Bu)] (**6**), is evident on the basis of the ^{31}P and ^{195}Pt NMR data (no signals for ^{27}Al NMR) in comparison to the spectra of the known compounds of analogue structure. Complex **6** rather rapidly transforms into the platinum alkyl/hydride isomer **7** in solution. Because of the similar time scales of the formation of **6** and the consecutive reaction and the very slow crystallisation from the reaction solution, it was impossible to obtain pure samples of **6** or **7** for further analytical characterisation. Unfortunately, we were not lucky again to obtain a perfect 1:1 mixed crystal as in the case of **3** and **4**, whatever we tried. Most interestingly, the reaction of [(dcpe)Pt(H)(CH_2*t*-Bu)] with $Al(CH_2SiMe_3)_3$

gave no hints at all for the formation of a Pt–Al product compound of the formula [(dcpe)Pt{Al(CH_2SiMe_3)$_2$}(CH_2SiMe_3)] (**8**). Instead the formation of a mixture of two different Pt–H species of so far unknown structure, was observed by in situ ^{31}P NMR spectroscopy.

2.2. Spectroscopic characterization

Pt–E compounds. Table 1 summarises the ^{31}P and the ^{195}Pt NMR spectroscopic data of all new compounds presented in this study. Similar to the data found for **1** and **2** the ^{31}P NMR spectrum of (dcpe)Pt[Ga(CH_2SiMe_3)$_2$](CH_2SiMe_3) (**3**) shows two sets of singlets with ^{195}Pt satellites at 76.6 ($J_{Pt-P(cis)}$ = 2589 Hz) and 66.4 ($J_{Pt-P(trans)}$ = 1594 Hz). These can be assigned to the two phosphorous atoms in *cis* and *trans* position of the nearly square planar platinum compounds, regarding the ER_2 ligand. As expected and in contrast to the starting compound [(dcpe)Pt(H)(CH_2t-Bu)] (δ = 76.6, $^1J_{Pt-P(cis)}$ = 1655 Hz; 63.7, $^1J_{Pt-P(trans)}$ = 1799 Hz, $^2J_{P-H(trans)}$ = 195 Hz) no coupling $^2J_{P-H}$ was observed for compound **3**. The expected coupling $^2J_{P-P}$ could not be resolved for any of the complexes. The phosphorous coupled ^{195}Pt{^{1}H} NMR spectrum of **3** displays a doublet of doublets at about δ −4735 and the values for the coupling constants $^1J_{Pt-P}$ are consistent with the respective ^{31}P NMR data.

Similar to the signals observed for Pt–Ga compound **3** the ^{31}P NMR spectrum of {(dcpe)Pt[In(CH_2t-Bu)$_2$](CH_2t-Bu)} (**5**) shows two sets of singlets with ^{195}Pt satellites at 75.9 ($J_{Pt-P(cis)}$ = 1788 Hz) and 73.6 ($J_{Pt-P(trans)}$ = 1691 Hz). The ^{195}Pt {^{1}H} NMR spectrum of **5** shows a doublet of doublets at δ −4611 which is in good agreement with the chemical shift observed for the gallium neopentyl compound **1** (δ −4687).

In analogy to the data found for compounds **1** and **5** the ^{31}P NMR spectrum of the crude product obtained from the reaction of [(dcpe)Pt(H)(CH_2t-Bu)] and Al(CH_2t-Bu)$_3$ after the evaporation of all volatile substances shows two sets of singlets with ^{195}Pt satellites at 74.6 ($J_{Pt-P(cis)}$ = 3158 Hz) and 66.1 ppm ($J_{Pt-P(trans)}$ = 1222 Hz). In the ^{195}Pt NMR spectrum of **6** a doublet of doublets was observed at δ −4970. These date support the existence of the complex (dcpe)Pt[Al(CH_2t-Bu)$_2$](CH_2t-Bu) (**6**). Longer reaction times or attempts to crystallize the isolated crude product at room temperature in a glove box over days led to a consecutive reaction and the formation of a second species **7**. This compound seems to exhibit a Pt–H bond, based on the NMR data, and thus a structure similar to the gallium compound **4**. The spectra of **7** are discussed below together with the data for the corresponding gallium monosyl compound **4**.

Pt-hydride compounds. ^{31}P and ^{195}Pt NMR data of the H-bridged compound {(dcpe)Pt(μ_2-H)[$CH_2Si(CH_3)_2$ $CH_2Ga(CH_2SiMe_3)_2$]} (**4**) were obtained from a sample of the complete amount of substance, from which the crystals for the X-ray analysis originated, after evaporation of all volatiles and resolution in C_6D_6. These data were compared with a sample obtained by prolonged heating of a mixture of [(dcpe)Pt(H)(CH_2t-Bu)] and Ga(CH_2SiMe_3)$_3$ after complete consumption of the starting platinum complex. The NMR data of the sample from which the crystals originated confirmed a composition of the substance of **3** and **4** in a relation of about 1:1 in full agreement with the composition of the unit cell of the crystal structure. Besides the signals of compound **3** (see Table 1) the proton coupled ^{31}P NMR spectrum reveals another singlet with ^{195}Pt satellites at δ 74.6 ($J_{Pt-P(cis)}$ = 1857 Hz) and a doublet with ^{195}Pt satellites at 65.6 ($J_{Pt-P(trans)}$ = 2679 Hz). For the signal at δ 65.6 coupling constant $^2J_{P-H(trans)}$ of 133 Hz was observed, typical for platinum hydride compounds. As the ^{31}P NMR data of [(dcpe)Pt(H)(CH_2SiMe_3)] (δ = 76.7, $^1J_{Pt-P(cis)}$ = 1994 Hz; 63.7, $^1J_{Pt-P(trans)}$ = 1779 Hz) are known by literature [16], the formation of this compound by simple alkyl substitution could be clearly ruled out. The ^{195}Pt {^{1}H} NMR spectrum of **4** displays a doublet of doublets at δ −5004 whereas the values for the coupling constants $^1J_{Pt-P}$ are again consistent with the respective ^{31}P NMR data. In the corresponding

Table 1
^{31}P and ^{195}Pt NMR spectroscopic data for complexes **3**–**7**[a]

Complex	^{31}P NMR (δ,$^1J_{Pt-P}$/Hz, $^2J_{P-H}$/Hz)			^{195}Pt NMR (δ, $^1J_{Pt-P}$/Hz, $^1J_{Pt-H}$/Hz)		
3	76.6 (s),	2589,	–	−4735 (dd),	2580,	–
	66.4 (s),	1594,	–		1584	
4	74.6 (s),	1857,	–	−5004 (dd),	1867,	866
	65.6 (s),	2679,	133		2670	
5	75.9 (s),	1788,	–	−4611 (dd),	1777,	–
	73.6 (s),	1691,	–		1691	
6	74.6 (s),	3158,	–	−4970 (dd),	3268,	–
	66.1 (s),	1222	–		1204	
7	72.4 (s),	1548,	–	−4974 (dd),	1515,	[b]
	64.0 (s),	2842,	128		2831	

[a] Recorded in C_6D_6.
[b] The coupling constant $^1J_{Pt-H}$ could not be determined, as a mixture of **6** and **7** was measured, which caused superpositions of the relevant signals.

proton and phosphorous coupled ^{195}Pt NMR spectrum a doublet of doublet of doublets is observed indicating a Pt–H coupling referring to a Pt–H bond. The signals for **3** and **4** are distinctly separated in the ^{195}Pt NMR spectrum and the coupling constant $^{1}J_{Pt-H}$ of 866 Hz could be clearly designated.

As mentioned above, the reaction of [(dcpe)Pt(H)(CH_2t-Bu)] and Al(CH_2t-Bu)$_3$ led to the formation a compound of the proposed formula {(dcpe)Pt[Al(CH_2t-Bu)$_2$](CH_2t-Bu)} (**6**) followed by the facile transformation into a consecutive species **7** within some days of storage of a solution of **6** in benzene at room temperature. Besides the signals of compound **6** the ^{31}P NMR spectrum of that mixture reveals a singlet with ^{195}Pt satellites at δ 72.4 ($J_{Pt-P(cis)}$ = 1548 Hz) and a doublet with ^{195}Pt satellites at 64.0 ($J_{Pt-P(trans)}$ = 2842 Hz, $^{2}J_{P-H(trans)}$ 128 Hz) assigned to a Pt–H species **7** (Fig. 1).

The ^{195}Pt {^{1}H} NMR spectrum of the mixture displays a doublet of doublets at δ −4970 assigned to **6**

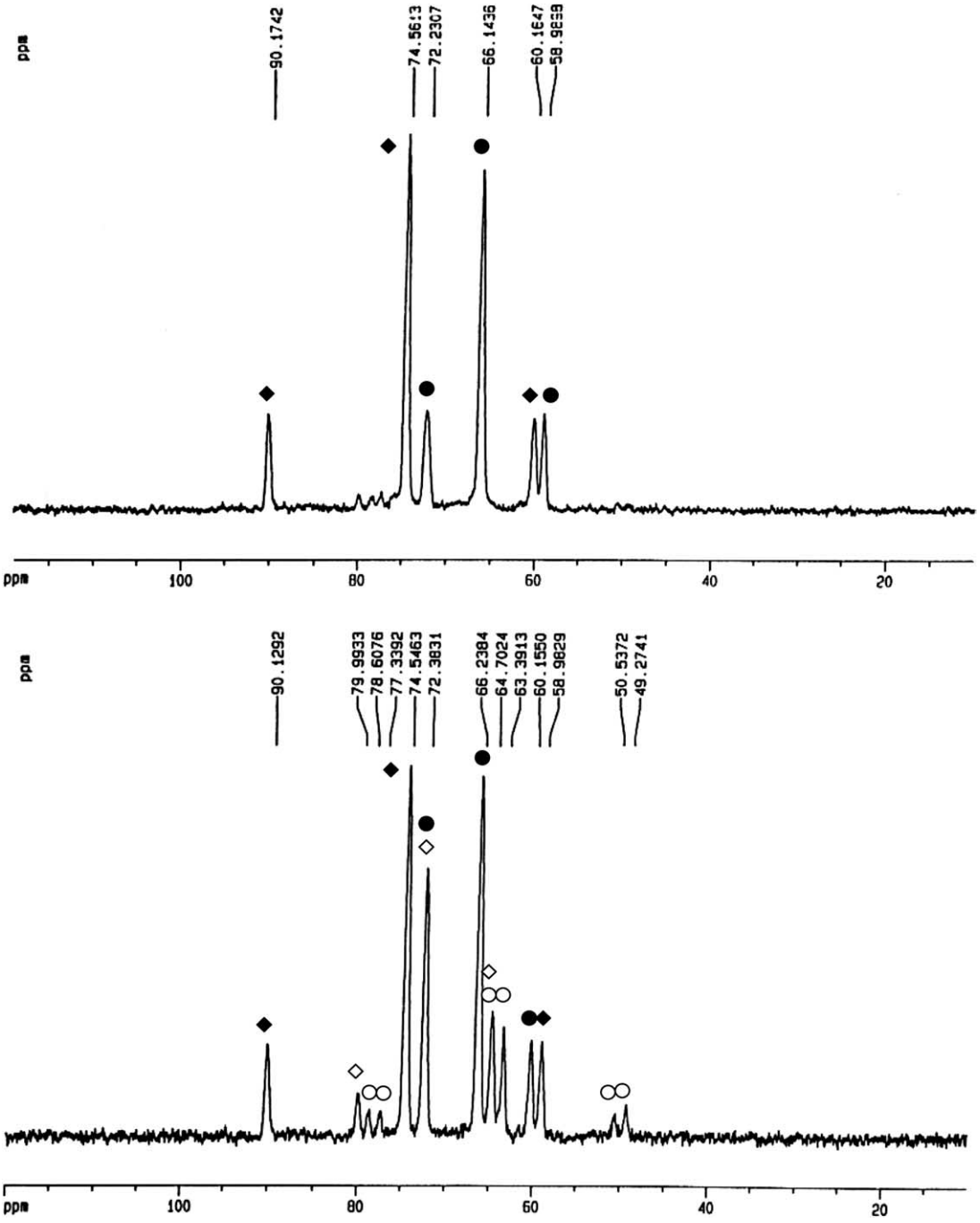

Fig. 1. ^{31}P NMR spectra of **6** (above) and a mixture of **6** and **7** (below). See Table 1 for the assignment: **6**, labels ♦ and •; 7 labels ◇ and ○○.

Table 2
Summary of crystal structure data for complexes **3**, **4** and **5**

	3 and **4**	**5**
Empirical formula	$C_{38}H_{81}GaP_2PtSi$	$C_{41}H_{81}InP_2Pt \cdot C_6H_6$
Molecular weight	949.07	1024.05
Crystal size (mm)	$0.24 \times 0.18 \times 0.15$	$0.28 \times 0.20 \times 0.15$
Crystal colour, habit	Colourless needles	Yellow rhombus
Crystal system	Triclinic	Triclinic
Space group	$P\bar{1}$	$P\bar{1}$
Unit cell dimensions		
a (Å)	14.27(2)	11.120(2)
b (Å)	16.26(2)	12.066(2)
c (Å)	21.14(2)	20.239(3)
α (Å)	76.64(2)	83.725(2)
β (Å)	71.9(2)	83.537(2)
γ (Å)	89.65(2)	65.201(2)
V (Å^3)	4529(8)	2443.5(5)
$\rho_{calc.}$ (g cm^{-3})	1.356	1.386
Z	4 ($2 \times$ **3**+$2 \times$ **4**)	2
μ(Mo Kα) (mm^{-1})	3.853	3.425
F(000)	1864	1044
θ range for data collection (°)	$1.91 < \theta < 25.72$	$1.86 < \theta < 27.57$
Reflections collected	19353	15155
Unique reflections	14873	10792
R_{int}	0.0443	0.0961
Observed reflections	11333	8880
No. of parameters	833	469
Final R[a]	0.0545	0.0838
R_w[b]	0.1387	0.2588
GooF	1.032	1.373
Residual extrema in final diff. map (e Å^{-3})	2.662 to −2.046	5.122 to −6.621
Diffractometer used	Bruker-axs-SMART 1000, Graphit-Monochromator	
Programs used	SHELXS-97, SHELXL-97	
Structure refinement	Full-matrix least-squares on F^2	

[a] $R = \sum|F_o - F_c|/\sum|F_o|$.
[b] $R_w = [\sum w(F_o^2 - F_c^2)^2/\sum w(F_o)^2]$.

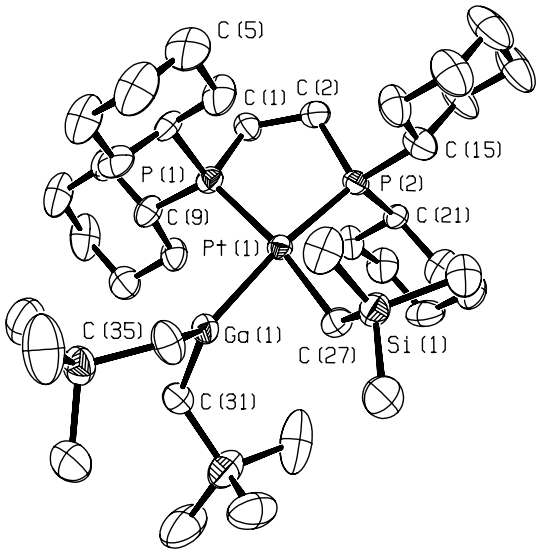

Fig. 2. Molecular structure of {(dcpe)Pt[Ga(CH_2SiMe_3)$_2$](CH_2-$SiMe_3$)} (**3**) in the solid-state (ORTEP drawing, the thermal ellipsoids are shown at the 50% level).

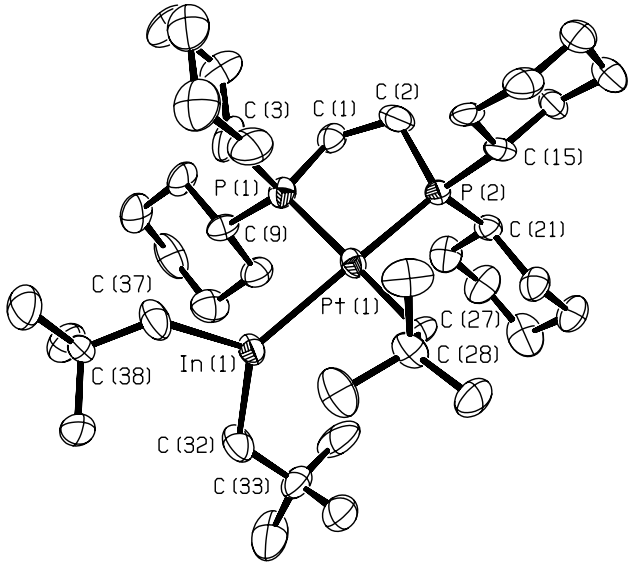

Fig. 3. Crystal structure of {(dcpe)Pt[In(CH_2t-Bu)$_2$](CH_2t-Bu)} (**5**) in the solid-state (ORTEP drawing, the thermal ellipsoids are shown at the 50% level).

and another one at δ −4974 assigned to **7**. The values for the coupling constants $^{1}J_{Pt-P}$ are in agreement with the respective ^{31}P NMR data. In the corresponding ^{195}Pt NMR spectrum again a multiplet is observed, indicating a further Pt–H coupling referring to a Pt–H bond of compound **7**. However, the superposition of the ^{195}Pt NMR signals for **6** and **7** did not allow a satisfying determination of the coupling constant $^{1}J_{Pt-H}$. These NMR data at least represent a hint for the possible formation of a hydridic species of the composition {(dcpe)Pt(μ_2-H)[$CH_2C(CH_3)_2CH_2Al(CH_2t\text{-}Bu)_2$]} (**7**) with a structure being probably similar to the structure observed for compound **4**.

2.3. Crystal structure analysis

2.3.1. Discussion of the structural features of the new Pt–E complexes 3 and 5

The crystallization of a mixture of {(dcpe)Pt[$Ga(CH_2SiMe_3)_2$](CH_2SiMe_3)} and {(dcpe)Pt(μ_2-H)[$CH_2Si(CH_3)_2CH_2Ga(CH_2SiMe_3)_2$]} (**3** and **4** Fig. 2, Table 3) resulted in the formation of colourless needles (mixed crystal of **3** and **4,** triclinic space group P). Compound {(dcpe)Pt[$In(CH_2t\text{-}Bu)_2$]($CH_2t\text{-}Bu$)} (**5**, Fig. 3, Table 4) crystallizes as yellow rhombs (**5**) in the triclinic space group P (Table 2). The molecular structures of **3** and **5** are as expected and quite comparable to the structures of the homologous complexes {(dcpe)Pt[$Ga(CH_2t\text{-}Bu)_2$]($CH_2t\text{-}Bu$)} (**1**) and {(dcpe)Pt[$In(CH_2SiMe_3)_2$] (CH_2SiMe_3)} (**2**) [1,2]. They are derived from the basic square planar structure of the starting compound [(dcpe)Pt(H)($CH_2t\text{-}Bu$)] by a exchange of the neopentyl and hydride ligands by the ER_2 and R units.

Coordinative environment of the Pt centre. The five-membered ring structure of the platinum diphosphine chelate unit of the starting compound is retained within the products. The platinum centres of **3** and **5** are coordinated in a distorted square planar mode by two phosphine ligands, an alkyl group (monosyl or neopentyl) and the group 13 dialkyl unit ER_2 (E = Ga, In; R = CH_2SiMe_3, CH_2t-Bu). The deviations of the atoms E(1) and C(27) from co-planarity regarding the plane defined by Pt(1), P(1) and P(2) are of marginal order. This is also revealed by the angular sums around the Pt centres. They are almost 360° in both cases. The cyclohexyl substituents are slightly bent backwards. As this was also found in the case of the sterically less crowded starting compound, the intramolecular interactions with the sterically demanding ER_2 units seem not to be the determining factor for this observation. The Pt(1)–C(27) bond length of 2.133(9) Å (**3**) and 2.137(9) Å (**5**) are in the typical range of Pt–C bonds and nearly identical with the Pt–C bond length of 2.125(5) Å in the starting compound [(dcpe)Pt(H)(CH_2zt-Bu)]. An interesting feature is the significant *trans*-influence of the ER_2 units on the Pt–P_{trans} bond length. The gallium compounds **1** and **3** exhibit a Δ(Pt–$P_{cis/trans}$) of about 0.070 (± 0.005) Å and the indium congeners **2** and **5** show a smaller difference of 0.037 (± 0.005) Å. The longer Pt–P_{trans} bonds expectedly correspond to smaller ^{1}J(Pt–P_{trans}) coupling constants (see Table 1). The Pt-Al complex **6** exhibits the smallest ^{1}J(Pt–P_{trans}) of 1222 Hz which should correspond to a value of Δ(Pt–$P_{cis/trans}$) > 0.070 Å (as observed for **1** and **2**). But unfortunately structural data for **6** could not be obtained.

Coordinative environment of the group 13 metal centres. The environment of the Ga and In centers of compounds **3** and **5** is strictly planar, as was also found for complexes **1** and **2**. The angular sums around the Ga and In centres are 360° in both cases. The Ga and In atoms lie within the planes C(31)–C(35)–Pt(1) (**3**) and C(32)–C(37)–Pt(1) (**5**), respectively. Due to the different steric requirements and the difference of the Pt–E and E–C bonds, the angles between the ligators (Pt, C, C) at the group 13 metal centre deviate from the ideal trigonal planar symmetry: the angles C–E–C amount to 111.5(5)° (**3**) and 112.8(5)° (**5**) (**1**: 116.7(6)°; **2**: 103.0(1)°). The angles C–E–Pt amount to 123.1(3) and 125.1(4)° for (dcpe)Pt[$Ga(CH_2SiMe_3)_2$](CH_2SiMe_3) and 118.9(4) and 127.7(4)° for {(dcpe)Pt[$In(CH_2t\text{-}Bu)_2$] (CH_2t-Bu)} (**1**: 121.4(5) and 121.8(4)°; **2**: 133.71(8) and 123.06(8)°).

Torsion of the plane ER_2 relative to the plane P_2Pt. The orientation of the plane ER_2 relative to the plane P_2–Pt is also a relevant feature. The Pt–Ga complex **3** (monosyl) exhibits a dihedral angle P(1)–Pt(1)–Ga(1)–C(31) of 89.4° quite different from **1** (neopentyl) with 123.4°. For the Pt–In compound **5** (neopentyl) a dihedral angle P(1)–Pt(1)–In(1)–C(32) of 107.3° has been

Table 3
Selected bond distances (Å) and bond angles (°) of compound **3**

Pt(1)–Ga(1)	2.376(2)	P(1)–Pt(1)–P(2)	86.9(1)
Pt(1)–P(1)	2.214(3)	Ga(1)–Pt(1)–C(27)	73.2(3)
Pt(1)–P(2)	2.290(3)	P(1)–Pt(1)–Ga(1)	97.66(8)
Pt(1)–C(27)	2.133(9)	P(2)–Pt(1)–C(27)	102.5(3)
Ga(1)–C(31)	1.98(1)	P(1)–Pt(1)–C(27)	170.5(3)
Ga(1)–C(35)	1.97(2)	P(2)–Pt(1)–Ga(1)	171.91(6)
Ga(1)···C(27)	2.694	Pt(1)–Ga(1)–C(31)	123.1(3)
P(1)–C(1)	1.82(1)	Pt(1)–Ga(1)–C(35)	125.1(4)
P(2)–C(2)	1.865(9)	C(31)–Ga(1)–C(35)	111.5(5)

Table 4
Selected bond distances (Å) and bond angles (°) of compound **5**

Pt(1)–In(1)	2.608(1)	P(1)–Pt(1)–P(2)	86.7(1)
Pt(1)–P(1)	2.265(3)	In(1)–Pt(1)–C(27)	90.4(3)
Pt(1)–P(2)	2.295(3)	P(1)–Pt(1)–In(1)	88.46(8)
Pt(1)–C(27)	2.137(9)	P(2)–Pt(1)–C(27)	95.2(3)
In(1)–C(32)	2.23(2)	P(1)–Pt(1)–C(27)	175.8(3)
In(1)–C(37)	2.22(1)	P(2)–Pt(1)–In(1)	168.78(8)
In(1)···C(27)	3.382	Pt(1)–In(1)–C(32)	127.7(4)
P(1)–C(1)	1.83(2)	Pt(1)–In(1)–C(37)	118.9(4)
P(2)–C(2)	1.90(2)	C(32)–In(1)–C(37)	112.8(5)

found which is different from the value of 93.6° for **2** (monosyl). The variation of the orientation of the ER_2 units within the solid-state structure may be related mainly to the steric influence of the organic ligand at the group 13 metal centre regarding the minimization of the steric repulsion between R and the cyclohexyl groups of the phosphine ligand as well as being controlled by the packing of the molecules in the crystal. However, electronic reasons may be important to some extent, too (i.e., Pt–E back bonding, see below).

The Pt–E bond. The Pt–Ga bond length of **3**of 2.376(2) Å is somewhat shorter compared to the situation in compound **1** (2.438(1) Å), the only other example of a Pt–Ga compound containing a Ga centre in a formal oxidation state of +III. For comparison, the Pt–Ga bond length of the complexes $[(dcpe)Pt(GaR)_2]$ ($R = Cp^*$, $C(SiMe_3)_3$) and $[Pt_2(\mu_2\text{-}GaCp^*)_3(GaCp^*)_2]$ with the Ga^I ligand and coordination numbers (CN) at the Ga centre 4 and 5 (if the Cp^* ligand is counted with a CN of 3) display a range between 2.315(1) and 2.465(1) Å [10a,b,e]. The estimated sum of the covalent radii in complex **3** amounts to 2.59–2.65 Å, while the shortest Pt–Ga distances in Pt/Ga phases were reported to lie around 2.45 Å [17]. However, the Pt–In distance of 2.608(1) of complex **5** is identical with the Pt–In bond length in $\{(dcpe)Pt[In(CH_2SiMe_3)_2](CH_2SiMe_3)\}$ (2.601(0) Å) [2], but longer in comparison to the complexes $\{Pt[InC(SiMe_3)_3]_4\}$ [10c] and $[(dcpe)Pt(InCp^*)_2]$ [10b] with In^I centres displaying Pt–In bond lengths in a range of 2.441(2)–2.569(1) Å.

2.3.2. Discussion of the structural features of the H-bridged complex *4*

It has already been mentioned, that in the particular sample successfully used for growing crystals of complex **3** the actual single crystal diffraction study surprisingly revealed the coexistence of **3** and $\{(dcpe)Pt(\mu_2\text{-}H)[CH_2Si(Me)_2CH_2Ga(CH_2SiMe_3)_2]\}$ (**4**), in the unit cell of the crystal. The H atom attached to the Pt centre is also quite close to the Ga centre and could be found in the difference fourier synthesis and its position was freely refined (see Fig. 4, and Table 5).

Coordinative environment of the platinum centre. The coordination of the Pt centre of **4** closely resembles the square plane arrangement of the parent complex $[(dcpe)Pt(H)(CH_2t\text{-}Bu)]$. The angular sum around the Pt(2) centre amounts to 358° (the Pt and Ga atoms of **4** were denoted by the index (2) in order to differentiate them from the metal centres Pt(1) and Ga(1) of compound **3** present within the same unit cell). The conformation of the $H–Pt–CH_2–Si(Me)_2–CH_2–Ga(CH_2SiMe_3)_2$ moiety created by the H atom bridging the Pt(2) and the Ga(2) atom resembles a twisted arrangement (Fig. 5). The bridging Pt–H distance of 1.75(10) Å exceeds distinctly the one reported for the terminal Pt–H bond of $[(dcpe)Pt(H)(CH_2t\text{-}Bu)]$ (1.56(5) Å) [14].

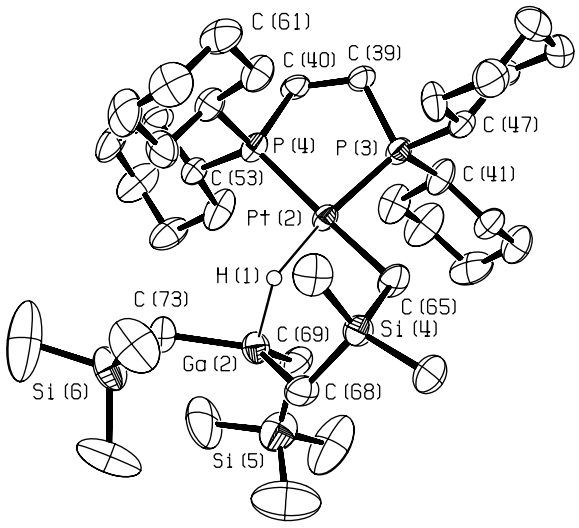

Fig. 4. Molecular structure the H-bridged Pt/Ga complex **4** of a co-crystallized sample of **3** and **4**. Both complexes **3** (see Fig. 2) and **4** were found within the unit cell in a relation of 1:1. (ORTEP drawing, the thermal ellipsoids are shown at the 50% level).

Table 5
Selected bond distances (Å) and bond angles (°) of compound **4**

Pt(2)–H(1)	1.75(10)	C(65)–Pt(2)–H(1)	80(3)
Pt(2)···Ga(2)	3.084(3)	P(3)–Pt(2)–P(4)	87.9(1)
Pt(2)–P(3)	2.204(3)	P(3)–Pt(2)–C(65)	92.3(3)
Pt(2)–P(4)	2.226(3)	P(4)–Pt(2)–H(1)	98(3)
Pt(2)–C(65)	2.084(9)	P(3)–Pt(2)–H(1)	170(3)
Ga(2)–H(1)	1.83(10)	P(4)–Pt(2)–C(65)	173.3(3)
Ga(2)–C(68)	2.00(1)	C(68)–Ga(2)–H(1)	83(3)
Ga(2)–C(69)	2.00(2)	C(69)–Ga(2)–H(1)	120(3)
Ga(2)–C(73)	1.97(1)	C(73)–Ga(2)–H(1)	94(3)
P(3)–C(39)	1.824(9)	C(68)–Ga(2)–C(69)	114.1(5)
P(4)–C(40)	1.833(9)	C(68)–Ga(2)–C(73)	122.8(5)
Pt(2)–H(1)–Ga(2)	119(3)	C(69)–Ga(2)–C(73)	116.1(5)

Coordinative environment of the Ga centre. The coordinative environment of the Ga centre is almost planar but may be also described as a base centred tetrahedron in comparison to regular tetrahedral gallanates like $K[Ga(CH_2SiMe_3)_3H]$ [18,19] with a angular sum of 333.9° regarding the three alkyl groups. The three C_α atoms of the alkyl substituents of **4**, C(68), C(69) and C(73) surround the Ga(2) centre in a nearly trigonal plane fashion, leading to a angular sum of 353° as it is

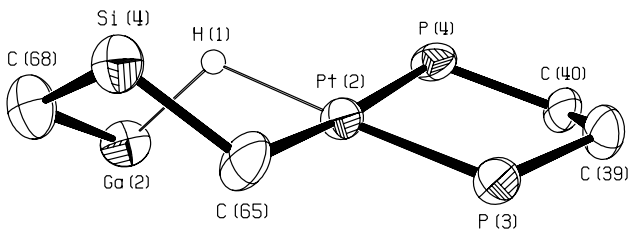

Fig. 5. The twisted conformation of the $H–Pt–CH_2–Si(Me)_2–CH_2–Ga(CH_2SiMe_3)_2$ moiety of compound **4**.

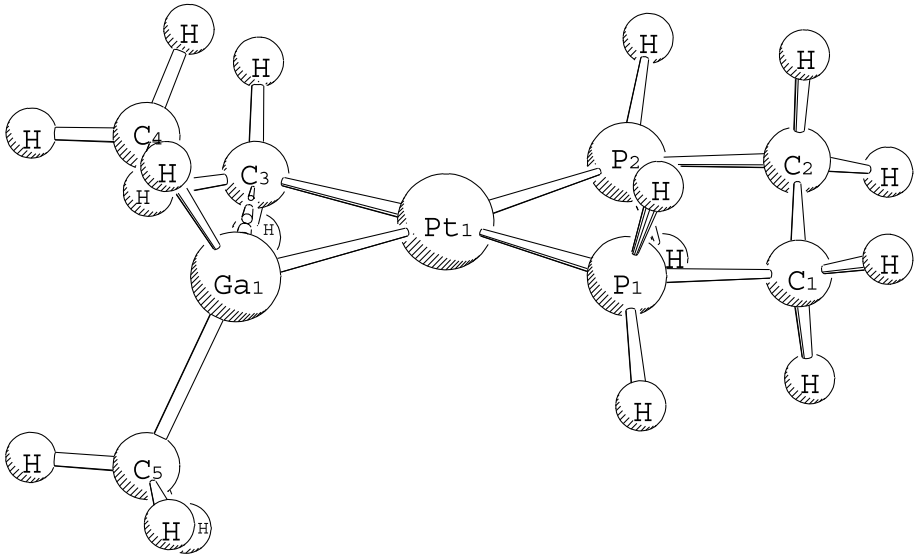

Fig. 6. Calculated structure of the model compound **1M** (SCHAKAL plot).

Table 6
Selected bond distances (Å) and bond angles (°) of model compound [(dhpe)Pt($GaMe_2$)(Me)] **1M**

Pt(1)–Ga(1)	2.444	P(1)–Pt(1)–P(2)	85.24
Pt(1)–C(3)	2.156	P(2)–Pt(1)–C(3)	103.04
Pt(1)–P(1)	2.285	P(1)–Pt(1)–C(3)	171.63
Pt(1)–P(2)	2.426	P(1)–Pt(1)–Ga(1)	104.39
Ga(1)–C(4)	2.006	P(2)–Pt(1)–Ga(1)	170.24
Ga(1)–C(5)	2.006	Pt(1)–Ga(1)–C(4)	121.55
Ga(1)···C(3)	2.253	Pt(1)–Ga(1)–C(5)	121.09
Ga(1)–Pt(1)–C(3)	67.37	C(4)–Ga(1)–C(5)	117.35

observed for the free tris(trimethylsilylmethyl)gallium [20]. Apparently the coordinative influence of the H atom on the GaR_3 unit as a donor is rather weak. In comparison to the Ga–H distance of 1.494 Å reported for $K[Ga(CH_2SiMe_3)_3H]$ the Ga–H distance of 1.83(10) Å of compound **4** is significantly longer. However, the Ga–H distance still lies within the region expected for neutral H-bridged gallium compounds [21]. The particular conformation of the six membered heterocycle defined by Pt(2), C(65), Si(4), C(68), H(1) and the angle Ga(2)–H(1)–Pt(2) of 119(3)° may be consequence of intramolecular steric restraints as well as crystal packing effects. However, we did not attempt to elucidate this issue in detail (see Fig. 6).

3. Theoretical calculations on the model compound {(dhpe)-Pt[$Ga(CH_3)_2$](CH_3)} 1M

The complexes of the type [(dcpe)Pt(ER_2)(R)] reveal a formally empty p-acceptor orbital p_x(E) at the group 13 metal centre. For this reason it seems to be interesting to elucidate the possibility of the presence of Pt–E dπ–pπ interactions. A comparison could be drawn to the isovalence electronic platinum silylene complex fragment $[(PCy_3)_2(H)Pt{=}Si(SEt)_2]^+$ reported by Tilley and co-workers [22,23] some time ago with an as well nearly orthogonal arrangement of the $Si(SR)_2$ and the L_3Pt plane. Theoretical calculations on the basis of this system reveal a good overlap of the Si_π orbital and the Pt orbitals of suitable symmetry. However, no significant *population* of the π bond has been found (the low valent Si centre is rather stabilized by π donation from the S atoms). Our L_3 Pt–ER_2 species does not posses π-donor ligands at the group 13 metal centre E. So, the contribution of some Pt → E back donation is a reasonable question, similarly to the situation of the silylene complex $[Cp^*(PMe_3)_2Ru{=}SiMe_2]BPh_4^F$ [22]. However, the characterization of the Pt–E bonding situation affords a detailed qualitative and quantitative analysis of this problem via modern quantum chemical methods.

We selected the model complex [(dhpe)Pt($GaMe_2$)(Me)] **1M** (dhpe = 1,2 diphosphinoethane), in which the cyclohexyl groups have been replaced by H atoms and the neopentyl or monosyl moiety by a methyl ligand (Me) for a first step towards more detailed quantum chemical calculations. The geometry of **1M** was optimised with the DFT functional BP86, SVP basis sets and a relativistic pseudopotential for Pt (Fig. 5, Table 6) [24–32].

The comparison of the calculated interatomic distances and angles (Table 6) shows that the structural data of **1M** are in reasonable agreement with the observed values for complex **1** [1]. The angular sums around the Pt- and the Ga centre of **1M** amount to exactly 360° each, so that the metal centres are both coordinated in a perfect plane mode. The dihedral angle of the P_2Pt-plane and the $GaMe_2$-plane is 88.4–91.5°

(P(1)–Pt(1)–Ga(1)–C(4) and P(1)–Pt(1)–Ga(1)–C(5), respectively). Apparently, there is no significant intramolecular steric hindrance between the dhpe ligand and the $GaMe_2$ moiety, thus, it can be concluded that complexes of this type prefer an orthogonal arrangement of the planes when steric restrictions are excluded.

There is one surprising feature of the model complex **1M** worth mentioning: the short distance Ga(1)···C(3) of 2.253 Å. In contrast, the estimated sum of the covalent radii is about 2.05 Å and compares with the bonding Ga–C distances of the compound {(dcpe)Pt[Ga(CH_2t-Bu)$_2$](CH_2t-Bu)} (**1**) are 2.00(1)–2.02(1) Å. However, in contrast to the model **1M**, complex **1** exhibits a typical non-bonding distance Ga···C(27) of 3.149 Å [1]. For the Pt–In compounds **5** the distances In–$C_{bonding}$ of 2.215–2.217 Å and In···$C(27)_{non\text{-}bonding}$ of 3.218 Å were found and **2** reveals quite similar data: In–$C_{bonding}$ = 2.22(1)–2.23(2) Å, In··· $C(27)_{non\text{-}bonding}$ = 3.382 Å. Interestingly, the complexes **1**, **2** and **5** are all stable against the rearrangement observed for **3** and supposed for **6** and **7** involving the particular E–C bonds and leading to the hydridic isomers. However, complex **3**, which transforms into **4**, exhibits an unusually short distance Ga(1)···C(27) of 2.694 Å. The dihedral angle between the Ga(CH_2SiMe_3)$_2$ moiety and the P_2Pt plane is close to 90°. This situation is quite similar to the features found for **1M**. The structural similarity between **3** and **1M** regarding the coordination of the GaR_2 moieties lead us to the speculation, that the optimized structure of the model compound **1M** could be regarded as a late transition state on the path to the insertion of the Pt centre of L_2Pt into the Ga–C(3) bond of a ER_3 unit. From this perspective an aspect regarding the reactivity of the sterically less demanding group 13 trialkyls towards the [L_2Pt] fragment becomes obvious. An oxidative addition would be less effective in these cases as compared with other possibilities, such as alkyl exchange reaction seems to be favoured. From this point of view a high steric demand of the alkyl ligands at the group 13 metal center seems to be a stringent requirement for the stabilisation of this type of compounds.

The bonding situation within the model compound **1M** was analysed by the Natural Bond Orbital method (Table 7). As expected, a relatively high partial charge of +1.15 at the group 13 metal centre E of the Pt–Ga bond represents a indication for an oxidation state of the Ga atom of rather +III. The GaR_2-fragment carries a weak positive charge (0.13), the Pt center (−0.10) as well as the fragment [(dhpe)Pt(Me)] (−0.13) carry a weak negative charge. The p(π)-population at the Ga atom reveals a negligible order of magnitude of the back-donation E ← Pt of 0.09 electrons in comparison to the net charge transfer of 0.21 electrons via σ-donation E → Pt.

The Wiberg bond index P(Pt–Ga) of 0.48 refers to nearly half a single bond, similar to the situation in the Pt–Ga compounds of the type [(dcpe)Pt(ER_2)$_2$]. Presumably as well a certain covalent part (shared electron) as a donor–acceptor interaction contribute to the bond formation.

4. Conclusions

We reported the synthesis and spectroscopic characterization of bimetallic compounds of the type [(dcpe)Pt(ER_2)(R)] (E = Ga, R = CH_2SiMe_3; E = Al, In, R = CH_2t-Bu). The crystal structures of the corresponding Pt–Ga and Pt–In compounds show the expected square plane geometry. The Ga and especially the Al complex show an interesting reactivity regarding consecutive reactions yielding a hydride bridged Pt/E species that could be verified by ^{31}P and ^{195}Pt NMR, IR as well as by a crystal structure analysis in the case of the Pt/Ga complex. A brief quantum-chemical analysis on the structure and bonding situation of the model complex [(dcpe)Pt(EMe_2)(M)] revealed no significant back-bonding from the transition metal to the gallium centre.

Table 7
NBO analysis of [(dhpe)Pt($GaMe_2$)(Me)] on the BP86/SVP level[a]

E	q[(dhpe)Pt(Me)]	q(Pt)	q(E)	q(Me)	p_x(E)[b]	p_y(E)[b]	p_z(E)[b]	Δq(E)[d]	Δq_π(E)[d]	Δq_σ(E)[d]	Δq(Me)[d]	P(Pt–E)
Ga	−0.13	−0.10	1.15	−0.51	0.13	0.29	0.46	0.12	−0.09	+0.21	0.01	0.48
			Free $GaMe_2$ fragment[c]									
			1.03	−0.52	0.04	0.24	0.42					

[a] Partial charges q, p-orbital populations, difference of the p-populations charges of the complexes and the free $GaMe_2$ fragment (calculated as a radical) Dq, Wiberg bond index P.
[b] p(π) AO of E.
[c] Values for the free $GaMe_2$ fragment, calculated in the geometry of the complexes.
[d] Negative values represent a higher electronic charge, and positive values represent a lower electronic charge in the complex relative to the free $GaMe_2$ fragment.

5. Experimental

5.1. General procedures

All manipulations were carried out under purified Ar atmosphere using standard vacuum techniques. The solvents were distilled over sodium and stored over molecular sieves prior to use. Procedures described in the literature were followed for the preparation of [(dcpe)Pt(H)(CH_2t-Bu)] [15], $Ga(CH_2SiMe_3)_3$ [33] and $In(CH_2t\text{-}Bu)_3$ [34]. Elemental analysis were performed by the Microanalytical Laboratory of the Ruhr-Universität Bochum. The NMR spectra were recorded in benzene-d_6 at 298 K using a Bruker Avance DPX-250 spectrometer (^{1}H, 250.1 MHz; ^{13} C, 62.9 MHz; ^{31}P, 101.3 MHz). Chemical shifts were referenced to the solvent resonances (C_6D_6) as internal standards and orthophosphoric acid as external standard, respectively. Infrared spectra were recorded as KBr pellets using a Perkin–Elmer 1720 X FT-IR spectrometer. Absorptions are described as follows: strong (s), medium (m), weak (w), and shoulder (sh).

5.2. Preparation of complex 3

A sample of 100 mg (0.145 mmol) [(dcpe)Pt(H)(CH_2t-Bu)] and 192 mg (0.580 mmol) $Ga(CH_2SiMe_3)_3$ were combined and suspended in 0.4 mL of methylcyclohexane in an evacuated and sealed NMR tube. After the reaction mixture was heated 1 h at 85–90 ° C gas evolution stopped and the reaction was complete according to the ^{31}P NMR spectrum. The NMR tube was opened in the glove box, the content was transferred to a Schlenk tube and all volatile components were removed in vacuo, whereby the raw product could be obtained in quantitative yield. The resulting solid was re-crystallized by slow evaporation of a solution of **3** in acetone in the glove box to give colourless crystals. Few crystals suitable for crystal structure analysis have been obtained by re-crystallization in toluene at 30 °C within the time of a year. This slow crystallization is accompanied by a partial molecular rearrangement of the product **3** into the Pt-hydride species **4** and the crystal structure analysis revealed that **3** and **4** were coexisting in a 1:1 ratio in the elementary cell. The yield of the isolated pure, micro-crystalline product **3** obtained from flash crystallization from acetone: 78 mg (57%). Decomposition beginning at 110 °C. Anal. Calc. for **3**, $C_{38}H_{81}GaP_2PtSi_3$ (mol. wt. 949.07): C, 48.09; H, 8.60. Found: C, 47.80; H, 8.94. ^{1}H NMR: δ 0.31 (s, 2H, $(CH_3)_3SiCH_2$–Pt–), 0.41 (s, 9H, $(CH_3)_3SiCH_2$–Pt–), 0.54 (s, 18H, $[(CH_3)_3SiCH_2]_2Ga$–), 0.65 (s, 4H, $[(CH_3)_3SiCH_2]_2Ga$–), 1.03–2.30 (complex and broad superpositions, 48H, $Cy_2P(CH_2)_2PCy_2$). ^{13}C{^{1}H} NMR: δ 1.57 ($CH_3)_3SiCH_2$–Pt–, 3.75 $[(CH_3)_3SiCH_2]_2$-Ga–, 4.82 ($(CH_3)_3SiC_2$–Pt–P), 16.4, 16.7 ($[(CH_3)_3Si$-$CH_2]_2Ga$–), 26.7–37.5 (complex superpositions). ^{31}P NMR: δ 76.6 (s with ^{195}Pt satellites, $^1J_{P(cis)–Pt}$ = 2589 Hz), 66.4 (s with ^{195}Pt satellites, $^1J_{P(trans)–Pt}$ = 1594 Hz). ^{195}Pt{^{1}H} NMR: δ 4735 (dd, $^1J_{Pt–P}$ = 2580 and 1548 Hz, respectively). IR (KBr): 2931 (s), 2847 (s), 1977 (w, b), 1623 (w, b), 1444 (m), 1409 (w), 1257 (m, sh), 1238 (m), 1105 (m), 1082 (m), 1006 (m, b), 853 (s), 822(s), 743 (m), 529 (w). MS (EI) *m/z* 947 (2) [M^+], 861 (33) [$M^+ - CH_2SiMe_3$], 616 (64) [$M^+ - (CH_2SiMe_3) - Ga(CH_2SiMe_3)_2$], 243 (38) [$M^+ - (dcpe)Pt(CH_2SiMe_3)$], 99 (100) [$Me_2Ga^+$], 73 (86) [$SiMe_3$].

5.3. Preparation of complex 5 · C_6H_6

A sample of 100 mg (0.145 mmol) [(dcpe)Pt(H)(CH_2t-Bu)] is suspended in about 0.4 mL $In(CH_2t\text{-}Bu)_3$ in an evacuated and sealed NMR tube. After the reaction mixture was heated 3 h at 75–80 °C gas evolution stopped and the reaction was complete according to the ^{31}P NMR spectrum. The NMR tube was opened in the glove box, the content was transferred to a Schlenk tube and all volatile components were removed in vacuo, whereby the raw product could be obtained in quantitative yield. The resulting solid was re-crystallized by slow evaporation of a solution of **5** in benzene in the glove box to give yellow rhombic crystals. Yield of the isolated crystalline product **5** · C_6H_6: 113 mg (76%). Decomposition beginning at 100 °C. Anal. Calc. for **5** · C_6H_6, $C_{47}H_{87}InP_2Pt$ (mol. wt. 1024.05) C, 55.13; H, 8.56. Found: C, 54.85; H, 8.65. ^{1}H NMR: δ 1.20 (s, 2H, $(CH_3)_3CCH_2$–Pt–), 1.25 (s, 4H, $[(CH_3)_3CCH_2]_2In$–), 1.54 (s, 9H, $(CH_3)_3CCH_2$–Pt–) 1.61 (s, 18H, $[(CH_3)_3CCH_2]_2In$–), 1.25–2.40 (complex and broad superpositions, 48 H, $Cy_2P(H_2)_2PCy_2$). ^{13}C{^{1}H} NMR: δ 33.9 ($(CH_3)_3CCH_2$–Pt–), 36.02 ($[(CH_3)_3$-$CCH_2]_2In$–), 26.6–37.2 (complex superpositions). ^{31}P NMR: δ 75.9 (s with ^{195}Pt satellites, $^1J_{P(cis)–Pt}$ = 1788 Hz), 73.6 (s with ^{195}Pt satellites, $^1J_{P(trans)–Pt}$ = 1691 Hz). ^{195}Pt{^{1}H} NMR: δ 4611 (dd, $^1J_{Pt–P}$ = 1777 and 1691 Hz, respectively). IR (KBr): 2931 (s), 2847 (s), 1444 (m), 1410 (w), 1356 (w), 1261 (s), 1234 (w), 1097 (vs, b), 1021 (vs, b), 853 (w), 800 (s, b), 739 (w), 655 (w), 526 (w).

5.4. Preparation of complex 6

A sample of 100 mg (0.145 mmol) [(dcpe)Pt(H)(CH_2t-Bu)] and 70 mg (0.290 mmol) $Al(CH_2t\text{-}Bu)_3$ were combined and suspended in 0.4 mL of methylcyclohexane in an evacuated and sealed NMR tube. After the reaction mixture was heated 40 min at 75 ° C gas evolution stopped and the reaction contained a maximum amount of **6** according to the ^{31}P NMR spectrum. The

NMR tube was opened in the glove box, the content was transferred to a Schlenk tube and all volatile components were removed in vacuo, whereby the raw product could be obtained in quantitative yield. The resulting solid was re-crystallized by slow evaporation of a solution of **6** in benzene at room temperature in the glove box to give a colourless microcrystalline solid. Following ^{31}P NMR spectroscopy the crystallization is accompanied of a molecular rearrangement of **6** in significant amounts within some days for the benefit of a Pt-hydride species **7**. Hence for the collection of the preliminary data listed below the crude product (obtained from the freshly performed synthesis after evaporation of all volatile components) was used and no elemental analysis was performed. The wide conformity of the NMR data with the values found for compounds **1** and **5** can be regarded as a hint for the similarity of the products. No crystals suitable for a X-ray analysis could be obtained. Decomposition beginning at 80° C. ^1H NMR: δ 1.22 (s, 18H, $[(CH_3)_3CCH_2]_2Al$–), 1.51 (s, 9H, $(CH_3)_3CCH_2$–Pt–) 1.54 (s, 4H, $[(CH_3)_3CCH_2]_2In$–) 1.25–2.40 (complex and broad superpositions, 48H, $Cy_2P(CH_2)_2PCy_2$ and $(CH_3)_3CCH_2$–Pt–). ^{13}C $\{^1H\}$ NMR: δ 35.4 $[(CH_3)_3CCH_2]_2Al$–, 35.8 $(CH_3)_3CCH_2$–Pt–, 26.3–37.2 (complex superpositions). ^{31}P NMR: δ 74.6 (s with ^{195}Pt satellites, $^1J_{P(cis)–Pt} = 3158$ Hz), 66.1 (s with ^{195}Pt satellites, $^1J_{P(trans)–Pt} = 1222$ Hz). ^{195}Pt $\{^1H\}$ NMR: δ 4970 (dd, $^1J_{Pt–P} = 3286$ and 1204 Hz, respectively). ^{27}Al NMR (65.2 MHz, C_6D_6, 298 K) δ 315. IR (KBr): 2931 (s), 2847 (s), 1444 (m), 1413 (w), 1356 (w), 1261 (s), 1223 (w), 1101 (vs, b), 1017 (vs, b), 853 (w), 800 (s, b), 746 (w), 662 (w), 529 (w).

6. Supplementary material

Supplementary data are available from CCDC, 12 Union Road, Cambridge, CB2 1EZ, UK on request, or will be provided directly from the authors upon request.

Acknowledgements

The support of this work by the Degussa AG and the W.C. Heraeus GmbH is gratefully acknowledged. We also thank the Deutsche Forschungsgemeinschaft and the Fonds der Chemischen Industrie for financial support. RAF gratefully acknowledges the mentorship of his academic teachers, Prof. W.A. Herrmann and Prof. H.D. Kaesz.

References

[1] R.A. Fischer, H.D. Kaesz, S.I. Khan, H.-J. Müller, Inorg. Chem. 29 (1990) 1601.
[2] R.A. Fischer, J. Behm, J. Organomet. Chem. 413 (1991) C10.
[3] H.D. Kaesz, R.S. Williams, R.F. Hicks, J.I. Zink, Y.-J. Chen, H.-J. Müller, Z. Xue, D. Xu, D.K. Shuh, Y.K. Kim, N. J. Chem. 14 (1990) 527.
[4] R.A. Fischer, J. Weiß, Angew. Chem. 111 (1999) 3002; R.A. Fischer, J. Weiß, Angew. Chem. Int. Ed. Engl. 38 (1999) 2830, and references therein.
[5] J. Uddin, C. Boehme, G. Frenking, Organometallics 19 (2000) 571.
[6] C. Boehme, J. Uddin, G. Frenking, Coord. Chem. Rev. 197 (2000) 249.
[7] C. Boehme, G. Frenking, Chem. Eur. J. 5 (1999) 2184.
[8] C.L.B. Macdonald, A.H. Cowley, J. Am. Chem. Soc. 121 (1999) 12113.
[9] T. Steinke, A. Kempter, M. Cokoja, C. Gemel, R.A. Fischer, Eur. J. Inorg. Chem. (2004) 4161.
[10] (a) D. Weiß, T. Steinke, M. Winter, R.A. Fischer, N. Fröhlich, J. Uddin, G. Frenking, Organometallics 22 (2000) 4583; (b) D. Weiß, M. Winter, K. Merz, A. Knüfer, R.A. Fischer, N. Fröhlich, G. Frenking, Polyhedron 21 (2002) 535; (c) W. Uhl, S. Melle, Z. Anorg. Allg. Chem. 626 (2000) 2043; (d) C. Gemel, T. Steinke, M. Winter, R.A. Fischer, in press; (e) D. Weiß, M. Winter, R.A. Fischer, C. Yu, K. Wichmann, G. Frenking, Chem. Commun. 24 (2000) 2495.
[11] T. Steinke, C. Gemel, M. Winter, R.A. Fischer, Chem. Eur. J., submitted.
[12] T. Steinke, C. Gemel, M. Cokoja, M. Winter, R.A. Fischer, Angew. Chem. Int. Ed. 43 (2004) 2299.
[13] T. Steinke, Dissertation, Bochum 2004.
[14] T. Cadenbach, Ch. Gemel, R. Schmid, S. Block, R.A. Fischer, Dalton Trans. (2004) 3171.
[15] (a) M. Hackett, J.A. Ibers, P. Jernakoff, G.M. Whitesides, J. Am. Chem. Soc. 108 (1986) 8094; (b) M. Hackett, J.A. Ibers, G.M. Whitesides, J. Am. Chem. Soc. 110 (1988) 1436.
[16] M. Hackett, G.M. Whitesides, J. Am. Chem. Soc. 110 (1988) 1449.
[17] P. Guex, P. Feschote, J. Less Common Met. 46 (1976) 101.
[18] R.B. Hallock, O.T. Beachley Jr., Y.-J. Li, W.M. Sanders, M.R. Churchill, W.E. Hunter, J.L. Atwood, Inorg. Chem. 22 (1983) 3683.
[19] L. Gmelin, E.H.E. Pietsch, A. Kotowski, M. Becke-Goehring, Gmelin Handbuch der Anorganischen Chemie, 8. Aufl., Springer Berlin, Berlin, 1987.
[20] K.-D. Fuhrmann, F. Huber, Z. Naturforsch. 35b (1980) 1376.
[21] S. Konietzny, H. Fleischer, S. Parsons, C.R. Pulham, J. Chem. Soc. Dalton Trans. (2001) 304.
[22] S.D. Grumbine, T.D. Tilley, J. Am. Chem. Soc. 115 (1993) 7884.
[23] S.D. Grumbine, T.D. Tilley, F.P. Arnord, A.L. Rheingold, J. Am. Chem. Soc. 116 (1994) 5495.
[24] The DFT calculations were performed with the gradient-corrected exchange functional of Becke [20] and the correlation functional of Perdew [21] (BP86). The Ahlrichs SVP basis set was used throughout [22]. This basis set contains a quasi-relativistic pseudopotential for Pt [23] with a (7s6p5d) valence basis set in a [2111111/411/41] contraction especially optimized for the Ahlrichs SVP basis. Geometry optimizations were carried out using the RI approximation [24] as implemented in the Turbomole program package [25]. The NBO analysis [26] was carried out using Gaussian 98 [27]. All stationary points were characterized as minima by full calculation of the Hessian matrix.
[25] A.D. Becke, Phys. Rev. A 38 (1988) 3098.
[26] J.P. Perdew, Phys. Rev. B 33 (1986) 8822.
[27] A. Schäfer, H. Horn, R. Ahlrichs, J. Chem. Phys. 97 (1992) 2571.
[28] D. Andrae, U. Häuß ermann, M. Dolg, H. Stoll, H. Preuß, Theor. Chim. Acta 77 (1990) 123.
[29] K. Eichkorn, O. Treutler, H. Öhm, M. Häser, R. Ahlrichs, Chem. Phys. Lett. 240 (1995) 283.

[30] (a) R. Ahlrichs, M. Bär, M. Häser, H. Horn, C. Kölmel, Chem. Phys. Lett. 162 (1989) 165;
(b) O. Treutler, R. Ahlrichs, J. Chem. Phys. 102 (1995) 346.
[31] A.E. Reed, L.A. Curtiss, F. Weinhold, Chem. Rev. 88 (1988) 899.
[32] M.J. Frisch, G.W. Trucks, H.B. Schlegel, G.E. Scuseria, M.A. Robb, J.R. Cheeseman, V.G. Zakrzewski, J.A. Montgomery, R.E. Stratmann, J.C. Burant, S. Dapprich, J.M. Milliam, A.D. Daniels, K.N. Kudin, M.C. Strain, O. Farkas, J. Tomasi, V. Barone, M. Cossi, R. Cammi, B. Mennucci, C. Pomelli, C. Adamo, S. Clifford, J. Ochterski, G.A. Petersson, P.Y. Ayala, Q. Cui, K. Morokuma, D.K. Malick, A.D. Rabuck, K. Raghavachari, J.B. Foresman, J. Cioslowski, J.V. Ortiz, B.B. Stefanov, G. Liu, A. Liashenko, P. Piskorz, I. Komaromi, R. Gomberts, R.L. Martin, D.J. Fox, T.A. Keith, M.A. Al-Laham, C.Y. Peng, A. Nanayakkara, C. Gonzalez, M. Challacombe, P.M.W. Gill, B.G. Johnson, W. Chen, M.W. Wong, J.L. Andres, M. Head-Gordon, E.S. Replogle, J.A. Pople, Gaussian 98 (Revision A.1), Gaussian Inc., Pittsburgh, PA, 1998.
[33] O.T. Beachley, R.G. Simmons, Inorg. Chem. 19 (1980) 1021.
[34] O.T. Beachley, J.C. Pazik, Organometallics 7 (1988) 1516.